Supporting Information File
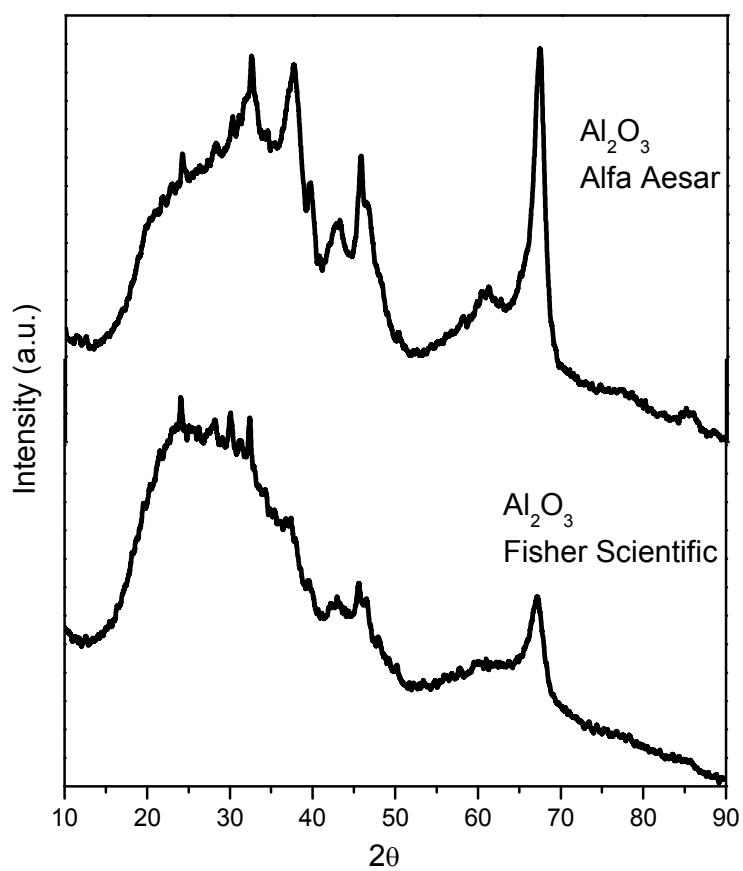

Figure 1S: Powder X-ray diffraction (XRD) patterns of the Al_2O_3 samples used in this study. XRD were collected by using a continuous scan mode from $2\theta = 10°$ to $90°$ with a step size 0.01.
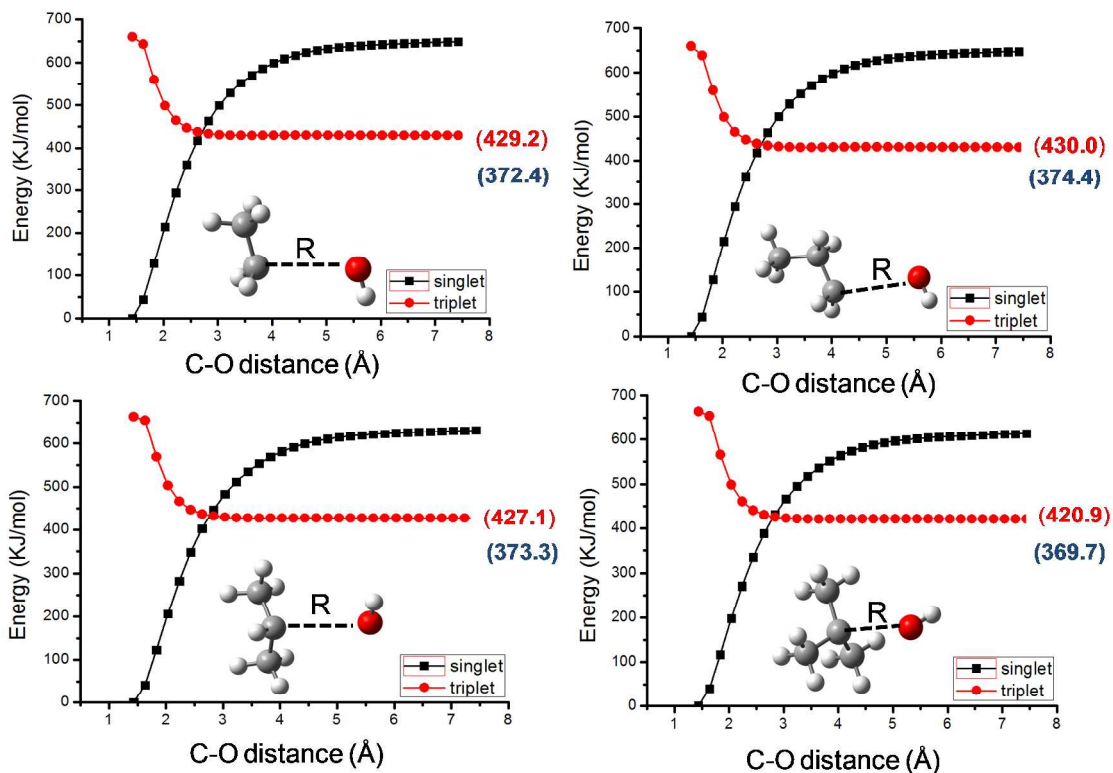
Figure 2S: Potential energy scan of the C-OH bond breaking under singlet and triplet spin states (electronic energies). All the curves are referenced to the corresponding alcohol ground state (E=0). The values in blue (appear also in Table 3 of the manuscript) are the enthalpies when the dissociated compounds are separated to infinity and fully relaxed (C_nH_{2n+1} + OH).
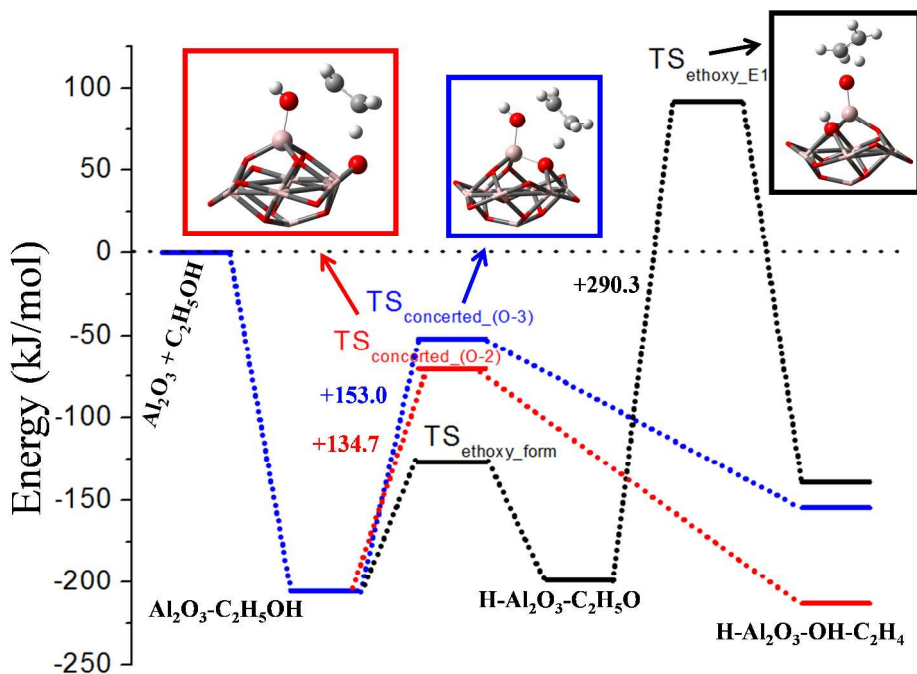
Figure 3S. DFT calculated paths considered for the dehydration of ethanol to ethylene on Al_8O_{12}. The E1 type mechanism through the alkoxy-intermediate exhibits a high barrier (290.3 kJ/mol) compared to the concerted dehydration mechanism (134.7 and 153.0 kJ/mol involving a 2- and 3-coordinated O atom, respectively).
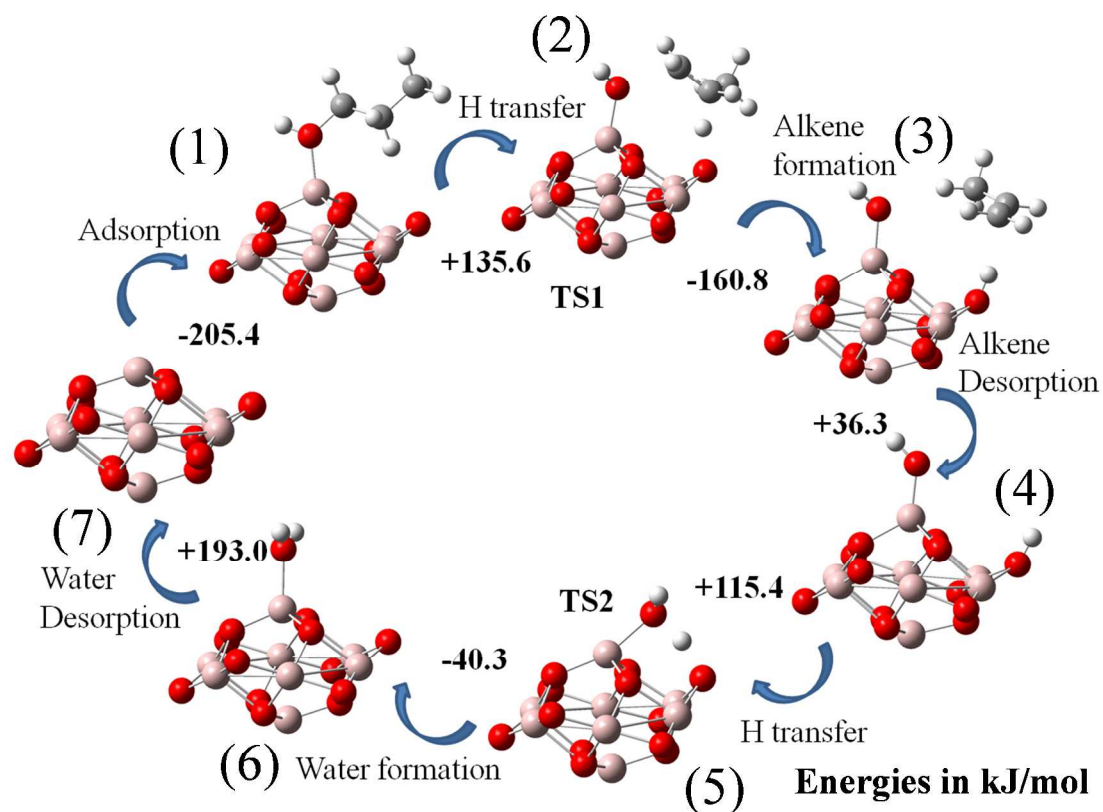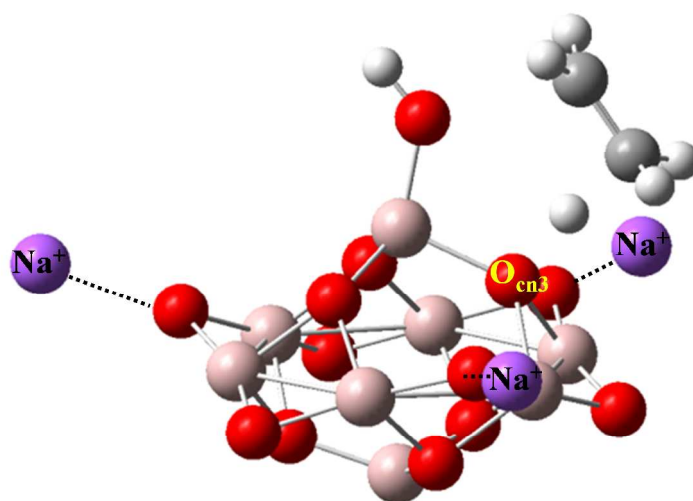
(1)

(2)

(3)

(4)

(5)

(6)

(7)

Adsorption

H transfer

Alkene formation

Alkene Desorption

H transfer

Water formation

Water Desorption

TS1

TS2

−205.4

+135.6

−160.8

+36.3

+115.4

−40.3

+193.0

Energies in kJ/mol

Figure 4S. Scheme of 1-propanol dehydration reaction involving a tri-coordinated Al Lewis-acid site and a two-coordinated O of γ-Al_2O_3 as presented in Figure 5 (b) of the manuscript. The steps are: 1) adsorption, 2) dehydration TS, 3) Alkene formation, 4) Alkene desorption, 5) water formation TS, 6) water formation, and 7) water desorption.

Alcohol	Distance (Angstroms)			Total charge on C_nH_{2n+1} and (OH) group (|e-|)		
	Non-adsorbed	Adsorbed	Transition State	Non-adsorbed	adsorbed	Transition State
Ethanol	R1=1.43 R2=1.09	R1=1.49 R2=1.09	R1=2.12 R2=1.28	+0.29 (OH:-0.29)	+0.44 (OH:-0.29)	+0.57 (OH:-0.56)
1-Propanol	R1=1.42 R2=1.09	R1=1.49 R2=1.09	R1=2.20 R2=1.26	+0.29 (OH:-0.29)	+0.40 (OH:-0.21)	+0.63 (OH:-0.57)
2-Propanol	R1=1.43 R2=1.09	R1=1.50 R2=1.09	R1=2.39 R2=1.21	+0.30 (OH:-0.30)	+0.45 (OH:-0.31)	+0.71 (OH:-0.61)
2-methyl-2-Propanol	R1=1.44 R2=1.09	R1=1.52 R2=1.09	R1=2.64 R2=1.16	+0.31 (OH:-0.31)	+0.50 (OH:-0.33)	+0.80 (OH:-0.65)

Table 1S. Structural and natural bond orbital (NBO) charge analysis of the alcohols in the gas-phase (non-adsorbed), adsorbed on the Al_8O_{12} cluster and at the transition state. R1 and R2 are the distances of C-OH and C-H, respectively, as they appear in Figure 5 (c) of the manuscript. R1 of all the alcohols is profoundly increased whereas R2 is much less at the transition state. This C-OH elongation induces a charge separation, giving carbenium ion characteristics to the transition state.

Base-site of Al_8O_{12}	Ea (kJ/mol)
$O_{CN=3}$ cluster doped with $3Na^+$	166.2
$O_{CN=3}$ undoped cluster	153.0
$O_{CN=2}$ undoped cluster	134.2

Figure 5S. Transition state of ethanol dehydration involving O_{cn3}, when the O_{cn2} sites of the cluster interact with Na^+. As it can be seen from the inset table, the alcohol dehydration barriers shift to higher energies with decreasing strength of the basic-center (O_{cn3} vs. O_{cn3}) and increasing Na^+ content (O_{cn3} on undoped vs. Na^+ doped Al_8O_{12}).
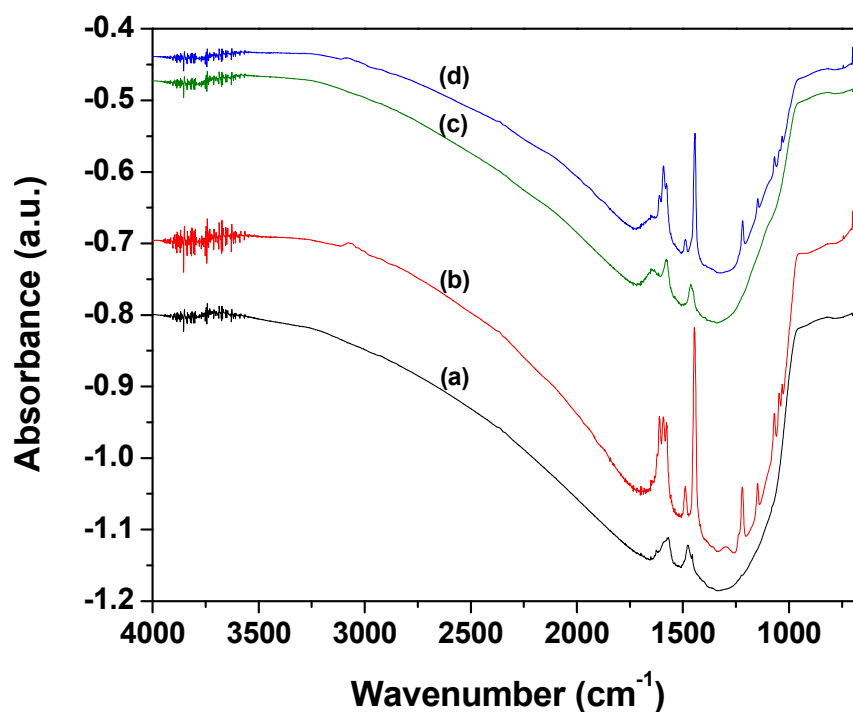
Figure 6S. FTIR spectra recorded at 30°C. All samples were treated in flowing dry air to 500°C in flowing dry air prior to degassing under vacuum (4.0 $*10^{-2}$ torr) for 1h.

(a) γ-Al_2O_3

(b) Pyridine (3 torr) was dosed at 30°C for 0.5h and the sample was subsequently degassed to 4.0 $*10^{-2}$ torr to remove physisorbed pyridine.

(c) The sample was exposed to water vapor (8.0 torr) at 300°C for 0.3h.

(d) Pyridine (2 torr) was dosed to the sample in (c) at 30°C for 0.5h, the sample was subsequently degassed to 4.0 $*10^{-2}$ torr to remove physisorbed pyridine.